Oxygen Isotope Effects on the Superconducting Transition and Magnetic States Within the Phase Diagram of $Y_{1-x}Pr_xBa_2Cu_3O_{7-\delta}$

R. Khasanov,[1,2,*] A. Shengelaya,[1,3] D. Di Castro,[1,4] E. Morenzoni,[2] A. Maisuradze,[1] I. M. Savić,[5] K. Conder,[6] E. Pomjakushina,[6,7] A. Bussmann-Holder,[8] and H. Keller[1]

[1]*Physik-Institut der Universität Zürich, Winterthurerstrasse 190, CH-8057 Zürich, Switzerland*
[2]*Laboratory for Muon Spin Spectroscopy, Paul Scherrer Institut, CH-5232 Villigen PSI, Switzerland*
[3]*Physics Institute of Tbilisi State University, Chavchavadze 3, GE-0128 Tbilisi, Georgia*
[4]*"Coherentia" CNR-INFM and Dipartimento di Fisica, Università di Roma "La Sapienza", P.le A. Moro 2, I-00185 Roma, Italy*
[5]*Faculty of Physics, University of Belgrade, 11001 Belgrade, Serbia*
[6]*Laboratory for Developments and Methods, Paul Scherrer Institute, CH-5232 Villigen PSI, Switzerland*
[7]*Laboratory for Neutron Scattering, Paul Scherrer Institute & ETH Zurich, CH-5232 Villigen PSI, Switzerland*
[8]*Max-Planck-Institut für Festkörperforschung, Heisenbergstrasse 1, D-70569 Stuttgart, Germany*

(Received 14 November 2007; published 11 August 2008)

The various phases observed in all cuprate superconductors [superconducting (SC), spin-glass (SG), and antiferromagnetic (AFM)] were investigated with respect to oxygen-isotope ($^{16}O/^{18}O$) effects, using here as a prototype system of cuprates $Y_{1-x}Pr_xBa_2Cu_3O_{7-\delta}$. All phases exhibit an isotope effect which is strongest where the respective phase terminates. In addition, the isotope effects on the magnetic phases (SG and AFM) are sign reversed as compared to the one on the superconducting phase. In the coexistence regime of the SG and SC phase a two-component behavior is observed where the isotope induced decrease of the superfluid density leads to a corresponding enhancement in the SG related density.

DOI: 10.1103/PhysRevLett.101.077001 PACS numbers: 74.72.Bk, 74.25.Dw, 76.75.+i

High-temperature cuprate superconductors (HTS's) exhibit a rich phase diagram as a function of doping. The undoped parent compounds are characterized by a long range 3D antiferromagnetic (AFM) order which is destroyed upon hole doping. Short-range AFM correlations survive, however, well in the superconducting (SC) region of the phase diagram by forming a spin-glass (SG) state, and SC and SG phases coexist within a limited doping range. Four phases can be thus differentiated: the AFM phase, the SG phase, the SG + SC phase, and the SC phase (see, e.g., Fig. 2). How these phases are related to each other is an open issue, and until now experiments are missing which could provide a fundamental link between them.

Isotope effects are a typical signature that lattice effects are involved in the respective electronic phase formation. While it is well known that in HTS's the isotope effect in the SC phase is strongly doping dependent—almost vanishing at optimum doping, but continuously increasing with decreasing doping [1–10]—very little was done in studying the isotope effect on the other phases. This includes only experimental investigations of the oxygen-isotope ($^{16}O/^{18}O$) effect (OIE) on the AFM ordering temperature (T_N) in undoped La_2CuO_4 [11] and the OIE on the SG ordering temperature (T_g) in Mn doped $La_{2-x}Sr_xCuO_4$ [12], as well as a theoretical investigation of the OIE on T_N [13].

Traditionally, isotope effects have played an important role for superconductivity since for conventional superconductors it was the *ultimate* proof that the lattice provides the glue to the electron pairing. Regarding the much more complex physics of HTS's as compared to conventional superconductors, the situation is not as easy to distinguish, since most BCS predictions are violated here. Besides the strongly doping dependent isotope effect on the superconducting transition temperature T_c [1–10], unexpected isotope effects on the in-plane magnetic penetration depth λ_{ab} [7–10], SG ordering temperature T_g [12], and the pseudogap onset temperature T^* were observed [14,15]. Interestingly, none of these isotope effects has been sufficiently convincing to consider seriously those theories where lattice effects are incorporated.

Here we report on oxygen-isotope experiments carried out in all the above phases (SC, SC + SG, SG, AFM) in order to demonstrate that the lattice plays an important and unconventional role in HTS's. We use $Y_{1-x}Pr_xBa_2Cu_3O_{7-\delta}$ (with δ close to zero) as a prototype of the HTS's since all the above phases are most easily accessible through variations of the Pr content x, i.e., from undoped to optimally doped. The OIE experiments were done by means of magnetization and muon-spin rotation (μSR) experiments, since these techniques have the advantage of being direct, bulk sensitive, and unambiguous. The OIE's on the AFM transition temperature T_N and the SG temperature T_g are sign reversed as compared to the one on T_c. In the SC and SG coexistence regime an interesting correlation between the respective isotope effects is observed which suggests that the involved superfluid and SG densities are correlated since the increase of one is at the expense of the other. This finding signifies that the same lattice effects are involved in both phase formations.

TABLE I. Summary of the OIE studies on T_c, T_g, and T_N for $Y_{1-x}Pr_xBa_2Cu_3O_{7-\delta}$. The meaning of the parameters is $^{16}T_x/^{18}T_x$ ($x = c, g, N$) and $^{16}(7-\delta)/^{18}(7-\delta)$: the transition temperatures and the oxygen content for the $^{16}O/^{18}O$ substituted samples, $\alpha_{T_c} = -d\ln T_c/d\ln M_O$, $\alpha_{T_g} = -d\ln T_g/d\ln M_O$, $\alpha_{T_N} = -d\ln T_N/d\ln M_O$: the OIE exponents of T_c, T_g, and T_N, respectively. The OIE exponents α_{T_c}, α_{T_g}, and α_{T_N} are not corrected for the ^{18}O exchange of 80(5)%.

x	$^{16}T_c$ (K)	$^{18}T_c$ (K)	α_{T_c}	$^{16}T_g$ (K)	$^{18}T_g$ (K)	α_{T_g}	$^{16}T_N$ (K)	$^{18}T_N$ (K)	α_{T_N}	$^{16}(7-\delta)$	$^{18}(7-\delta)$
0.00	91.19(5)	90.99(4)	0.018(5)	···	···	···	···	···	···	6.951(2)	6.953(2)
0.20	74.07(2)	73.27(2)	0.086(3)	···	···	···	···	···	···	···	···
0.30	57.97(8)	56.79(7)	0.163(15)	1.13(11)	1.66(12)	−3.8(1.2)	···	···	···	···	···
0.40	44.80(2)	43.25(3)	0.277(7)	7.07(9)	7.56(9)	−0.55(31)	···	···	···	6.929(3)	6.934(3)
0.45	36.50(6)	35.12(6)	0.302(19)	15.54(13)	16.58(11)	−0.54(9)	···	···	···	···	···
0.50	23.12(4)	20.16(4)	1.024(21)	17.82(11)	18.46(12)	−0.29(7)	···	···	···	···	···
0.55	14.4(2)	<1.7	7(1)[a]	21.05(18)	21.65(21)	−0.23(9)	···	···	···	6.953(2)	6.954(2)
0.58	···	···	···	22.8(2)	23.2(2)	−0.13(9)	···	···	···	···	···
0.65	···	···	···	32.3(4)	34.4(4)	−0.52(14)	···	···	···	···	···
0.70	···	···	···	···	···	···	100.5(1.4)	116.8(1.3)	−1.30(14)	6.946(3)	6.957(3)
0.80	···	···	···	···	···	···	210.2(4)	212.6(4)	−0.09(2)	···	···
1.00	···	···	···	···	···	···	283.2(7)	282.5(7)	0.02(3)	6.953(2)	6.949(3)
0.00	91.35(4)[b]	91.16(4)[c]	0.017(5)	···	···	···	···	···	···	···	···
0.40	44.63(3)[b]	43.25(3)	0.247(8)	7.10(9)[b]	7.56(9)	−0.52(30)	···	···	···	6.933(3)[b]	···

[a]Estimated value (see text)
[b]Back-exchanged $^{18}O \rightarrow {}^{16}O$ sample
[c]Back-exchanged $^{16}O \rightarrow {}^{18}O$ sample

Polycrystalline samples of $Y_{1-x}Pr_xBa_2Cu_3O_{7-\delta}$ ($0 \leq x \leq 1.0$) were prepared by standard solid state reaction [16]. Oxygen-isotope exchange was performed during heating of the samples in $^{18}O_2$ gas. To ensure the same thermal history of the substituted (^{18}O) and not substituted (^{16}O) samples, both annealings (in $^{16}O_2$ and $^{18}O_2$ gas) were always performed simultaneously. The ^{18}O content in the samples, as determined from a change of the sample weight after the isotope exchange, was found to be 80(5)% for all ^{18}O substituted samples. The total oxygen content (7-δ) of the samples with $x = 0.0$, 0.4, 0.55, 0.7, and 1.0 was determined by a high-accuracy volumetric analysis [16] (see Table I). We emphasize that the total oxygen contents of the $^{16}O/^{18}O$ substituted samples are the same within experimental errors, except for $x = 0.7$ where a small deviation is found.

The OIE on T_c was obtained by field-cooled magnetization (M_{FC}) experiments performed with a SQUID magnetometer in a field of 1.0 mT and at temperatures between 1.75 K and 100 K. The values of T_c were defined as the temperatures where the linearly extrapolated $M_{FC}(T)$'s intersect the zero line [see Fig. 1(a)]. The OIE's on the magnetic ordering temperatures (T_g and T_N) were extracted from the zero-field μSR data. No magnetism down to $T \simeq 1.7$ K was detected for the $^{16}O/^{18}O$ substituted samples with $x = 0.0$ and $x = 0.2$. For $x = 0.3$ and 0.4 magnetism was identified as a fast decrease of the asymmetry at $T < 10$ K and 5 K, respectively. For $x \geq 0.45$ damped oscillations due to muon-spin precession in local magnetic fields were observed. The μSR asymmetry spectra for $x = 0.8$ and 1.0, i.e., deep in the antiferromagnetic phase, were analyzed by using the following expression:

$$A(t) = A_n \exp(-\sigma^2 t^2/2) + A_m[\omega \exp(-\lambda_1 t)\cos(\gamma_\mu B_\mu t) + (1-\omega)\exp(-\lambda_2 t) J_0(\gamma_\mu B_\mu t)]. \quad (1)$$

Here A_m and A_n represent the oscillating and nonoscillating amplitudes, respectively, σ is the Gaussian relaxation rate, ω is a weighting factor, B_μ is the mean internal magnetic field at the muon site, $\gamma_\mu = 2\pi \times 135.5342$ MHz/T is the muon gyromagnetic ratio, and J_0 is the zeroth-order Bessel function. We used the damped Bessel function J_0 together with the cosine oscillating term in order to account for the unphysically large values of the

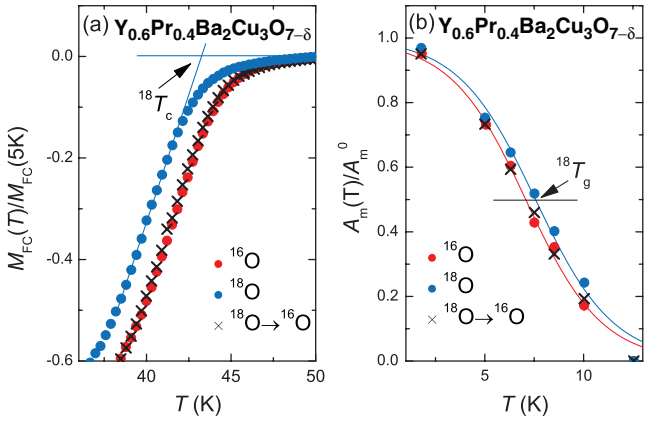

FIG. 1 (color). (a) Temperature dependences of the field-cooled magnetization M_{FC} normalized to its value at $T = 5$ K, and (b) A_m/A_m^0 for ^{16}O, ^{18}O, and back-exchanged $^{18}O \rightarrow {}^{16}O$ samples of $Y_{0.6}Pr_{0.4}Ba_2Cu_3O_{7-\delta}$. The solid lines in (b) were calculated by using Eq. (2). The arrows indicate T_c and T_g for the ^{18}O substituted sample.

initial phase $\phi \simeq 20°$–$45°$ which has to be introduced close to T_N in order to fit the data by using the cosine term only [$\cos(\gamma_\mu B_\mu t + \phi)$]. For $0.45 \leq x \leq 0.7$ and for $x = 0.4$ and 0.3 the analysis was simplified by taking from the second part of Eq. (1) only the damped Bessel term and the exponential damping term with $B_\mu = 0$, respectively. The magnetic ordering temperatures (T_g and T_N) were then determined by using the phenomenological function:

$$A_m(T)/A_m^0 = (1 + \exp[(T - T_{g,N})/\Delta T_{g,N}])^{-1}. \quad (2)$$

Here A_m^0 is the maximum value of the asymmetry and $\Delta T_{g,N}$ is the width of the magnetic transition [see Fig. 1(b)].

In order to exclude doping differences in the ^{18}O and ^{16}O samples to be the origin of shifts in the transition temperatures, back-exchange OIE experiments were carried through for $x = 0.0$ and $x = 0.4$. As shown in Fig. 1, the ^{16}O oxygen back-exchange of the ^{18}O sample of $Y_{0.6}Pr_{0.4}Ba_2Cu_3O_{7-\delta}$ results within error in almost the same $M_{FC}(T)$ [panel (a)] and $A_m(T)$ [panel (b)] as for the ^{16}O sample. The results of the OIE's on T_c, T_g, and T_N are summarized in Table I and Fig. 2. The doping dependences of T_c, T_g, and T_N for the ^{16}O substituted samples are in agreement with the results of Cooke *et al.* [17]. The second magnetic transition at $T_{N_2} \simeq 17$ K (observed for $x = 0.7$–1.0) associated with the ordering of the Pr sublattice is not considered here since this is not universal to cuprate families [18].

The OIE on the three transition temperatures, T_c, T_g, and T_N is defined in the standard way, i.e.,

$$\alpha_{T_{c,g,N}} = -\frac{d\ln T_{c,g,N}}{d\ln M_O} = -\frac{\Delta T_{c,g,N}/T_{c,g,N}}{\Delta M_O/M_O} = -\frac{(^{18}T_{c,g,N} - {}^{16}T_{c,g,N})/{}^{16}T_{c,g,N}}{(^{18}M_O - {}^{16}M_O)/{}^{16}M_O}, \quad (3)$$

where M_O is the mass of the oxygen isotope (^{16}O/^{18}O). The values of $\alpha_{T_{c,g,N}}$ are listed in Table I and shown in Fig. 3 as a function of Pr content x. For $0.0 \leq x \leq 0.5$ the values of α_{T_c} agree with previous results [2]. In order to estimate α_{T_c} for $x = 0.55$, we assume for $^{18}T_c$ the conservative value $^{18}T_c = 1.7(1.7)$ K, yielding $\alpha_{T_c} = 7(1)$ (which is not shown in Fig. 3). In the SG phase a high value of $\alpha_{T_g} = -3.8(1.2)$ for $x = 0.3$ was found. Note that similarly large values of $\alpha_{T_g} = -2.7$ to -6.0 were previously reported for Mn doped $La_{2-x}Sr_xCuO_4$ [12].

The observed OIE exponents α_{T_c}, α_{T_g}, and α_{T_N} exhibit unusual features. (i) All of them depend strongly on x, being small at $x = 0.0$ for T_c, $x \simeq 0.6$ for T_g, and $x = 1.0$ for T_N, and strongly increase upon approaching the value of x where the corresponding phase terminates (see solid lines in Fig. 3). For $0.5 \leq x \leq 0.55$, α_{T_c} exceeds considerably the BCS isotope exponent $\alpha_{T_c}^{BCS} = 0.5$. (ii) α_{T_c}, and both α_{T_g} and α_{T_N}, have *opposite* signs, i.e., T_c decreases with increasing oxygen-isotope mass ($^{16}T_c > {}^{18}T_c$), whereas T_g and T_N increase ($^{16}T_g < {}^{18}T_g$, $^{16}T_N < {}^{18}T_N$, except for $x = 1.0$). This is particularly interesting in the region of the phase diagram where superconductivity and SG magnetism coexist (see Figs. 2 and 3). (iii) The absence of an OIE on T_N in the undoped ($x = 1.0$) compound (see

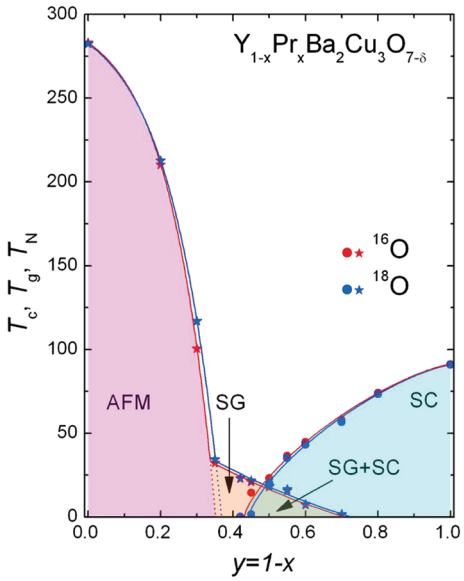

FIG. 2 (color). Dependence of T_c, T_g, and T_N for ^{16}O/^{18}O substituted $Y_{1-x}Pr_xBa_2Cu_3O_{7-\delta}$ on the Pr content $y = 1 - x$. The solid lines are guides to the eye. The areas denoted by AFM, SG, and SC represent the antiferromagnetic, the spin-glass, and the superconducting regions, respectively. SG + SC is the region where spin-glass magnetism coexists with superconductivity.

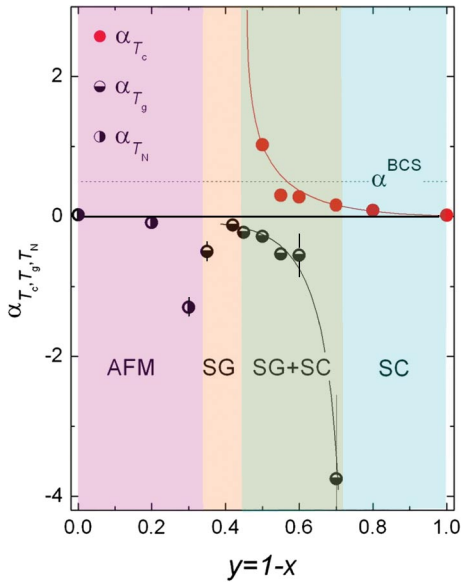

FIG. 3 (color). OIE exponents α_{T_c}, α_{T_g}, and α_{T_N} for ^{16}O/^{18}O substituted $Y_{1-x}Pr_xBa_2Cu_3O_{7-\delta}$ as a function of the Pr content $y = 1 - x$. The point $\alpha_{T_c} = 7(1)$ for $x = 0.55$ is not shown. The dashed line corresponds to $\alpha_{T_c}^{BCS} = 0.5$. The solid lines are guides to the eye. The meaning of the areas denoted by AFM, SG, SG + SC, and SC are the same as in Fig. 2.

Table I) suggests that the magnetic exchange energy J is unaffected by the isotope substitution. Simultaneously, it is intriguing to propose that J cannot be the source of the observed OIE's on T_N, T_g, and T_c in contrast to ideas of, e.g., Ref. [19].

In the coexistence regime of SC and SG an interesting anticorrelation between OIE's on T_c and T_g takes place which does not only refer to a sign reversal. In the regime where α_{T_g} is large, the OIE on T_c is small and vice versa (see Fig. 3). This finding suggests that this region of the phase diagram is phase separated. Note, however, that the absolute values of α_{T_c} and α_{T_g} differ considerably; i.e., a simple shift of the phase diagram to a different doping level cannot be done. If we assign for each doping level part of the electronic density to the SC and the remaining to the SG one, the change of the sign of the corresponding α (α_{T_c} vs α_{T_g}) and its reversal with respect to its magnitude find a natural explanation, namely, that the ^{18}O caused diminishing of the electron density participating in the pairing is accompanied by a corresponding increase in the electron density related to the SG state. Consequently, a relationship between both phases can be established which is novel and nontrivial. Since it has been shown that the isotope effect on T_c can be consistently explained through polaron formation [20], the same conclusion must be reached for the SG phase, at least in the region where both coexist. In the AFM regime also a reversal of α_{T_N} as compared to α_{T_c} is observed which seems to follow the one on T_g by reaching a maximum in magnitude at $x \simeq 0.7$ (see Fig. 3). If the onset of the AFM phase is related to the metal insulator transition, an explanation of the doping dependence can be achieved through polaron formation which renormalizes and reduces the single particle kinetic energy [20]. Thereby the metal insulator transition is shifted to higher temperatures in the ^{18}O system as compared to the ^{16}O one. For the undoped compound these effects are dying out and full 3D AFM order sets in.

In conclusion, the different phases observed in all cuprate superconductors were investigated with respect to OIE's by means of μSR and magnetization experiments. These techniques have the advantage of being direct, bulk sensitive, unambiguous, and able to measure T_c as well as T_g in the coexistence region. While the OIE's for the AFM, SG, and the SC phases are sign reversed with respect to each other, another anticorrelation is observed in the region where SC and SG phases coexist. Here a small OIE on T_c corresponds to a large OIE on T_g in sequence and vice versa. This behavior suggests that in this regime phase separation sets in where the superfluid density coexists with a SG related one. The diminishing of the electronic density assigned to the superfluid phase caused by isotope exchange results in an increase in the SG related density. Since the isotope effect on T_c can be accounted for by polaron formation [20], the one on T_g is expected to originate from the same physics. By relating the AFM transition temperature to the metal insulator transition, a reduction in kinetic energy caused by polaron formation explains this OIE as well. The various OIE effects reported here are clearly evidence that lattice effects are effective in all phases of HTS's imposing serious constraints on theories for cuprate superconductivity.

This work was partly performed at the Swiss Muon Source (SμS), Paul Scherrer Institute (PSI, Switzerland). The authors are grateful to K. Alex Müller for many stimulating discussions and to A. Amato, R. Scheuermann, and D. Herlach for providing instrumental support during the μSR experiments. This work was supported by the Swiss National Science Foundation, by the K. Alex Müller Foundation, and in part by the SCOPES Grant No. IB7420-110784, the EU Project CoMePhS, and the NCCR program MaNEP.

*rustem.khasanov@psi.ch

[1] B. Batlogg *et al.*, Phys. Rev. Lett. **59**, 912 (1987).
[2] J. P. Franck *et al.*, Phys. Rev. B **44**, 5318 (1991); J. P. Franck, in *Physical Properties of High Temperature Superconductors IV*, edited by D. M. Ginsberg (World Scientific, Singapore, 1994), pp. 189–293.
[3] D. Zech *et al.*, Nature (London) **371**, 681 (1994).
[4] G.-M. Zhao *et al.*, Nature (London) **385**, 236 (1997); G.-M. Zhao *et al.*, J. Phys. Condens. Matter **10**, 9055 (1998).
[5] G.-M. Zhao, H. Keller, and K. Conder, J. Phys. Condens. Matter **13**, R569 (2001).
[6] J. Hofer *et al.*, Phys. Rev. Lett. **84**, 4192 (2000).
[7] R. Khasanov *et al.*, J. Phys. Condens. Matter **16**, S4439 (2004).
[8] R. Khasanov *et al.*, Phys. Rev. Lett. **92**, 057602 (2004); R. Khasanov *et al.*, Phys. Rev. B **74**, 064504 (2006); R. Khasanov *et al.*, Phys. Rev. B **75**, 060505 (2007).
[9] H. Keller, in *Superconductivity in Complex Systems*, edited by K. A. Müller and A. Bussmann-Holder (Springer, Berlin, 2005), p. 143.
[10] J. L. Tallon *et al.*, Phys. Rev. Lett. **94**, 237002 (2005).
[11] G.-M. Zhao, K. K. Singh, and Donald E. Morris, Phys. Rev. B **50**, 4112 (1994).
[12] A. Shengelaya *et al.*, Phys. Rev. Lett. **83**, 5142 (1999).
[13] A. Bussmann-Holder, Int. J. Mod. Phys. B **12**, 3080 (1998).
[14] D. Rubio Temprano *et al.*, Phys. Rev. Lett. **84**, 1990 (2000).
[15] F. Raffa *et al.*, Phys. Rev. Lett. **81**, 5912 (1998).
[16] K. Conder, Mater. Sci. Eng., R **32**, 41 (2001).
[17] D. W. Cooke *et al.*, Phys. Rev. B **41**, 4801 (1990).
[18] Within our experimental accuracy no OIE on T_{N_2} was observed.
[19] R. Ofer *et al.*, Phys. Rev. B **74**, 220508(R) (2006).
[20] A. Bussmann-Holder and H. Keller, in *Polarons in Advanced Materials*, edited by A. S. Alexandrov (Springer, Dordrecht & Canopus Publishing Ltd., Bristol, 2007), p. 599.